Available online at www.sciencedirect.com
SCIENCE DIRECT®
Journal of Sound and Vibration 278 (2004) 327–342
JOURNAL OF SOUND AND VIBRATION
www.elsevier.com/locate/jsvi

Analytical approximation of the primary resonance response of a periodically excited piecewise non-linear–linear oscillator

J.C. Ji*, Colin H. Hansen

Department of Mechanical Engineering, The University of Adelaide, Adelaide, SA 5005, Australia

Received 6 March 2003; accepted 7 October 2003

Abstract

An analytical approximate solution is constructed for the primary resonance response of a periodically excited non-linear oscillator, which is characterized by a combination of a weakly non-linear and a linear differential equation. Without eliminating the secular terms, a valid asymptotic expansion solution for the weakly non-linear equation is analytically determined for the case of primary resonances. Then, a symmetric periodic solution for the overall system is obtained by imposing continuity and matching conditions. The stability characteristic of the symmetric periodic solution is investigated by examining the asymptotic behaviour of perturbations to the steady state solution. The validity of the developed analysis is highlighted by comparing the first order approximate solutions with the results of numerical integration of the original equations.

1. Introduction

Active magnetic bearings use magnetic force to suspend a rotor. The force generated by the magnetic actuator is inherently non-linear and is a function of the current in the stator coils and the position of the rotor. A magnetic bearing is required to provide a larger magnetic force to support the rotor when the rotor undergoes an unwanted larger amplitude motion. However, physical limitations, such as saturation, prevent the force increasing beyond some practical limit. Saturation phenomena may be manifested in a magnetic bearing as the saturation of the magnetic material, saturation of the power amplifier, and/or the limitation of the control current. It is of great interest to be able to determine the dynamical behaviour of a rotor suspended by a magnetic

*Corresponding author. Tel.: +61-8-8303-6941; fax: +61-8-8303-4367.
E-mail addresses: jcji@mecheng.adelaide.edu.au (J.C. Ji), chansen@mecheng.adelaide.edu.au (C.H. Hansen).

0022-460X/$ - see front matter
doi:10.1016/j.jsv.2003.10.022

bearing, as an accurate knowledge of this behaviour can be used in the design of actuators and in the fault diagnosis of the system.

Due to the weak non-linearity of magnetic force and the presence of saturation, the equations of motion governing a rotor that is suspended even in a single-degree-of-freedom magnetic bearing are non-linear with a piecewise non-linear–linear characteristic. It is well known in the context of non-linear oscillations [1–5] that the steady state response of a uniformly weakly non-linear oscillator could exhibit primary and secondary resonances phenomena, for which a small-amplitude excitation may produce a relatively large-amplitude response. For the non-smooth non-linear system considered here, which is mathematically modelled by a combination of a weakly non-linear and a linear differential equation, it is anticipated that such resonances may also occur in the steady state response of the system. Though the dynamics of piecewise linear systems has recently been an active topic of intensive research (see Refs. [6–16] and the references cited therein), the dynamics of a piecewise non-linear–linear system has not yet been reported in the literature, to the authors' knowledge.

This paper attempts to develop an approximate solution for the primary resonance response of a periodically excited non-linear–linear oscillator. Due to the force non-smooth non-linearity in the equations of motion, the usual perturbation method of seeking a steady state periodic solution for a uniformly non-linear system is not applicable to the non-smooth system considered here. An asymptotic expansion is instead used to give an approximate solution for the weakly non-linear differential equation, which does not need to eliminate the secular terms in the first order equation. The complete solution for the overall system comprises two parts, which correspond to the normal operating region and the saturation zone and join at the transition points of the force non-smooth non-linearities. More importantly, as will be seen, the first order approximate solution is capable of providing an excellent representation of the exact solution.

2. Equations of motion

The model considered here is a two-pole, single-degree-of-freedom magnetic bearing with a pair of opposed magnets in combination to provide forces, as discussed in Refs. [17,18]. This simple model, as shown in Fig. 1, represents the fundamental structure for many more complicated magnetic bearings.

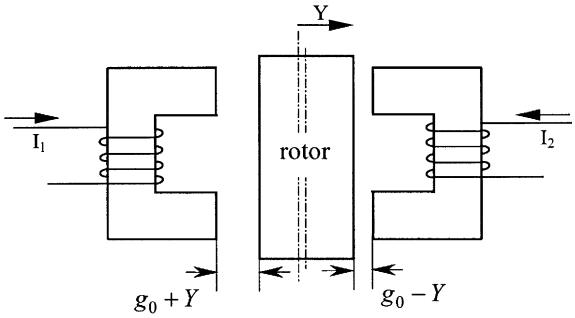

Fig. 1. A single-degree-of-freedom magnetic bearing.

The equations of motion for an unbalanced rigid rotor can be written as

$$MY'' = -CY' + F_{mb} + ME\Omega_0^2 \cos(\Omega_0 T), \tag{1}$$

where Y designates the displacement of the geometry centre of the rotor from the centre of magnetic bearing, M is the mass of the rotor, C is the damping coefficient, F_{mb} is the magnetic force, E is the mass unbalance eccentricity of the rotor, Ω_0 is the rotating speed of the rotor, and the prime indicates differentiation with respect to the physical time T.

In the presence of saturation, the net force resulting from the difference of attractive forces of the two electromagnets is assumed to have the following forms:

$$\begin{aligned} &\text{under normal operating conditions,} \quad F_{mb} = \frac{A_g}{\mu_0}(B_1^2 - B_2^2), \\ &\text{under the condition of saturation,} \quad F_{mb} = \pm f_{sat}, \end{aligned} \tag{2}$$

where μ_0 denotes the permeability of free space, A_g represents the projection area of the magnetic pole, B_1 and B_2 the magnetic flux density, and f_{sat} the maximum magnetic force. For simplicity, magnetic flux density and field density are assumed to be uniform through the iron core and air gap. Field fringing and leakage effects are neglected. The magnetic permeability within the iron core is considered to be very high (infinite) compared with the permeability in the air gap. The magnetic flux density in the air gaps is approximately of the form [19]

$$B_i = \frac{\mu_0 N_i I_i}{2g_i}, \quad i = 1, 2, \tag{3}$$

where N_i are the number of coil windings ($N_1 = N_2 = N$), I_i represent the current flowing in the coils, and g_i denote the air gap between the rotor and magnets. The current and the air gaps can be expressed as

$$\begin{aligned} &I_1 = \max(I_b + i_c, 0), \quad I_2 = \max(I_b - i_c, 0), \\ &g_1 = g_0 + Y, \quad g_2 = g_0 - Y, \end{aligned} \tag{4}$$

where I_b and i_c are the bias and control currents, respectively, and g_0 is the nominal air gap between the rotor and magnets. For simplicity, the feedback control system is assumed to generate a current that is proportional to the rotor displacement and velocity, i.e., a PD controller, with the form

$$i_c = k_p Y + k_d Y', \tag{5}$$

where k_p and k_d represent the proportional and derivative gains, respectively. As mentioned previously, saturation may occur in several ways and without loss of generality, it may be assumed that saturation takes place when $|k_p Y + k_d Y'| \geqslant I_b$.

Expanding the normal magnetic force in a Taylor series up to the third order about the nominal operating conditions $(Y, i_c) = (0, 0)$, and introducing the non-dimensional parameters $y = Y/g_0$, $t = \bar{\Omega} T$ in Eq. (1), yields the following equations of motion in non-dimensional form:

$$\ddot{y} + (c + d)\dot{y} + \omega^2 y + \alpha y^3 + (3d - 2pd)y^2\dot{y} - d^2 y\dot{y}^2 = F\cos\Omega t \quad \text{for } |y| \leqslant y_s, \tag{6a}$$

$$\ddot{y} + c\dot{y} + F_{sat}\,\mathrm{sgn}(y) = F\cos\Omega t \quad \text{for } |y| \geqslant y_s, \tag{6b}$$

where y is the dimensionless displacement of the rotor, the dimensionless proportional and derivative gains are defined as $p = k_p g_0/I_b$, $d = k_d g_0 \bar{\Omega}/I_b$, the dimensionless damping coefficient $c = C/(M\bar{\Omega})$, the dimensionless natural frequency $\omega^2 = p - 1$, the dimensionless forcing amplitude and frequency are given by $F = E\Omega_0^2/(g_0\bar{\Omega}^2)$, $\Omega = \Omega_0/\bar{\Omega}$, the dimensionless maximum magnetic force under saturation is $F_{sat} = (p^3 - 2p^2 + 3p - 2)/p^3$, and the dot represents the differentiation with respect to the non-dimensional time t, $\bar{\Omega}^2 = \mu_0 N^2 A_g I_b^2/(Mg_0^3)$, $\alpha = 3p - p^2 - 2$.

Here, for simplicity, the upper boundary of saturation zone is set to be approximately equal to $y_s = 1/p$ instead of $y_s = 1/p - (d/p)\dot{y}_s$, as the dimensionless derivative gain is much smaller than the proportional gain in physical systems.

Roughly speaking, the overall system given by Eq. (6) may admit two kinds of solutions, namely, a small-amplitude motion ($|y(t)| \leqslant y_s$), and a large amplitude motion ($|y(t)| \geqslant y_s$). For a small-amplitude motion ($|y(t)| \leqslant y_s$), the dynamic behaviour of the rotor is determined only by the solution of Eq. (6a). This kind of motion is not considered in the present paper as the steady state response can be easily obtained using the usual perturbation method [20–22]. To construct a solution for the large-amplitude response of the overall system, it is first necessary to seek the individual general solutions to Eqs. (6a) and (6b). Then the solutions are joined at the transition points of the non-smooth magnetic force by implementing an appropriate set of matching conditions. A general solution is easy to write out for the linear equation (6b). However, no exact analytical solution to Eq. (6a) is available so an approximate solution is sought instead.

3. Approximate analytical periodic solutions

This section presents a detailed analytical procedure for developing an approximate solution for the overall system. The analysis is based on the assumed existence of an asymptotic expansion solution for the weakly non-linear differential equation (6a) and an exact solution for the linear differential equation (6b). Then the approximate periodic solution for the overall system is obtained by imposing an appropriate set of periodicity and matching conditions. It is well known in the context of non-linear oscillations that primary resonances and secondary resonances (super-harmonic and sub-harmonic resonances) could occur in the steady state response of a uniformly non-linear system such as that characterized by Eq. (6a), when the natural frequency and forcing frequency satisfy a particular relationship. In the present paper, an approximate solution under the primary resonance conditions is sought using an asymptotic expansion.

For a large amplitude periodic response of the overall system given by Eq. (6), the motion will enter the saturation region at least once over one period. A typical example of a large-amplitude periodic motion will enter the saturation region twice over one period, which will be referred to here as a doubly entering saturation region per cycle of periodic motion. In this section, emphasis is placed on the analysis and description of such a symmetric motion, as shown in Fig. 2. The motion consists of four distinct segments according to the following four time intervals; $[t_0, t_1]$, $[t_1, t_2]$, $[t_2, t_3]$, $[t_3, t_4]$, where t_i denote the time instants that the non-smooth non-linearities of magnetic force take place. Due to the symmetry of the solution, only two parts of the motion need to be considered.

For the first segment of the motion, an approximate solution for the primary resonance response is sought using an asymptotic expansion method. To use a perturbation method, the

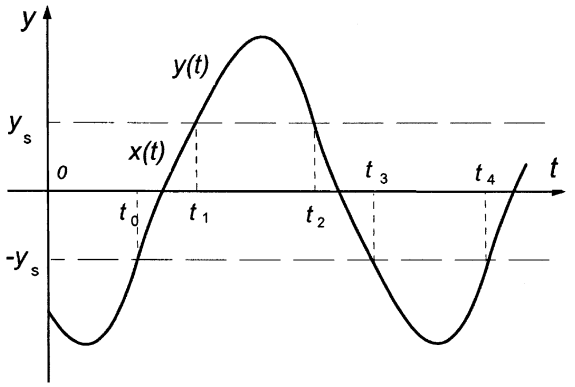

Fig. 2. A symmetric period-one motion with a doubly entering saturation zone per cycle; $x(t)$ denotes the segment of motion in the normal operating region $|x(t)|\leqslant x_s$, $y(t)$ represents the segment in the saturation region $|y(t)|\geqslant y_s$, t_0 denotes the starting time, and $t_i (i = 1, 2, 3, 4.)$ the time instants that the non-smooth non-linearities take place, $\pm y_s$ indicate the boundaries of saturation zone.

following variables are introduced: $y = \varepsilon^{1/2}x$, $c = \varepsilon\mu$, $d = \varepsilon\delta$, $f = \varepsilon^{3/2}F$, where ε is a book-keeping non-dimensional parameter. Then Eq. (6a) becomes

$$\ddot{x} + \varepsilon(\mu + \delta)\dot{x} + \omega^2 x + \varepsilon\alpha x^3 + \varepsilon^2\alpha_1 x^2\dot{x} + \varepsilon^3\alpha_2 x\dot{x}^2 = \varepsilon f\cos\Omega t \quad \text{for } |x|\leqslant x_s, \tag{7}$$

where $\alpha_1 = 3\delta - 2p\delta$, $\alpha_2 = -\delta^2$, $x_s = 1/(\varepsilon^{1/2}p)$.

It is assumed that an approximate periodic solution to Eq. (7) is a straightforward expansion asymptotic series with respect to powers of the small parameter ε [20–22]. The approximate solution to the first order for Eq. (7) is given by

$$x(t) = x_0(t) + \varepsilon x_1(t) \quad \text{for } |x(t)|\leqslant x_s, \tag{8}$$

where $x_0(t)$ and $x_1(t)$ are functions yet to be determined. The second and higher order terms are neglected in the asymptotic solution, although any desired higher order terms can be easily obtained using a similar procedure.

To avoid the appearance of the small divisor terms in the first order approximate solution in the vicinity of primary resonances, a detuning parameter is introduced according to

$$\omega^2 = \Omega^2 + \varepsilon\sigma, \tag{9}$$

where σ is the external detuning, which quantitatively describes the nearness of Ω to ω.

Substituting Eqs. (8) and (9) into Eq. (7) and equating the coefficients of like powers ε^0 and ε on both sides, leads to the following set of differential equations:

$$\ddot{x}_0 + \Omega^2 x_0 = 0, \tag{10}$$

$$\ddot{x}_1 + \Omega^2 x_1 = -(\mu + \delta)\dot{x}_0 - \sigma x_0 - \alpha x_0^3 + f\cos\Omega t. \tag{11}$$

It is easy to note that as a result of ordering, excitation, damping, and dominant non-linearity terms appear in Eq. (11). This indicates that the first order approximate solution could be capable of providing a valid representation of the exact solution for the case of primary resonances, as additional high order terms in the asymptotic expansion solution make a very small contribution

to the expansion solution. In fact, as will be seen, the first order asymptotic solution is an excellent approximation to the primary resonance response of the system.

The solution to the homogeneous linear equation (10) can be written as

$$x_0(t) = A_1 \sin \Omega(t - t_0) + B_1 \cos \Omega(t - t_0), \tag{12}$$

where A_1, B_1 and t_0 are constants to be determined. Substituting Eq. (12) into Eq. (11) and solving the resultant inhomogeneous equation gives rise to the general solution $x_1(t)$ as

$$\begin{aligned} x_1(t) = {} & l_1 \sin \Omega(t - t_0) + l_2 \cos \Omega(t - t_0) + k_1(t - t_0) \sin \Omega(t - t_0) + k_2(t - t_0) \cos \Omega(t - t_0) \\ & + f_1 t \sin \Omega t + k_3 \sin 3\Omega(t - t_0) + k_4 \cos 3\Omega(t - t_0), \end{aligned} \tag{13}$$

where the coefficients l_1, l_2, k_i and f_1 are defined in Appendix A. Here, it has been assumed that the steady state response starts at time instant t_0 from the initial condition $x(t_0) = -x_s$ and remains thereafter in the normal operating region $|x(t)| \leqslant x_s$ until moment t_1. Since the origin of the starting time has been set by a choice of the forcing term in Eqs. (13), it is not possible to set $t_0 = 0$. It is easy to see from Eq. (13) that three secular terms do not have enough time to grow and lead to an unbounded response in the steady state response, because both the time interval $(t_1 - t_0) \in (0, \pi/\Omega)$ and time $t \in [t_0, t_1]$ for undergoing this motion are finite and small. Thus, the nominal secular terms in the solution expressions need not be eliminated properly as is necessary when the usual perturbation method is applicable for seeking an approximate solution for a uniformly weakly non-linear equation [1–5].

For the second segment of the motion, the solution to the linear equation (6b) can be expressed in the form

$$y(t) = A_2 e^{-c(t-t_1)} + B_2 + m(t - t_1) + G \sin \Omega t + H \cos \Omega t \quad \text{for } |y(t)| \geqslant y_s, \tag{14}$$

where A_2, B_2 and t_1 are constants to be determined, $m = -F_{sat}\,\mathrm{sgn}(\dot{y})/c$, $G = cf/\Omega(c^2 + \Omega^2)$, $H = -f/(c^2 + \Omega^2)$.

At this point it is clear that there are six unknowns associated with the problem; that is, four constants A_1, B_1, A_2, B_2, and two crossing times t_0 and t_1. These constants can be determined by implementing an appropriate set of initial conditions as well as periodicity, continuity and symmetry conditions, which can be expressed as follows:

$$\begin{aligned} & x(t_0) = -x_s, \quad x(t_1) = x_s, \quad y(t_1) = \varepsilon^{1/2} x_s, \quad \dot{y}(t_1) = \varepsilon^{1/2} \dot{x}(t_1) \\ & y(t_2) = \varepsilon^{1/2} x_s, \quad \dot{y}(t_2) = -\varepsilon^{1/2} \dot{x}(t_0), \quad t_2 = \frac{\pi}{\Omega} + t_0. \end{aligned} \tag{15a–g}$$

Here, the last two conditions arise from the symmetry of the solution being examined. The four unknown constants A_i, B_i $(i = 1, 2)$ can be determined as functions of the system parameters and two crossing times t_0 and t_1 by imposing conditions (15a, c, e, f). Then substituting these constants into the corresponding solutions and imposing conditions (15b,d) yields a set of two transcendental equations for unknown t_0 and t_1 as follows:

$$\begin{aligned} & h_{11} S_{10} + h_{12} C_{10} + h_{13} \sin \Omega t_1 + h_{15} S_{30} + h_{16} C_{30} = x_s, \\ & h_{21} S_{10} + h_{22} C_{10} + h_{23} \sin \Omega t_1 + h_{24} \cos \Omega t_1 + h_{25} S_{30} + h_{26} C_{30} = m - cA_2, \end{aligned} \tag{16}$$

where the coefficients S_{10}, C_{10}, S_{30}, C_{30}, and h_{ij} are given in Appendix B.

Eq. (16) involves system parameters and two unknown crossing times t_0 and t_1 only. It is evident that no analytical solutions to Eq. (16) can be found, and thus numerical means have to be adopted to solve the crossing times for all possible solutions. The constants A_i, B_i $(i = 1, 2)$ can be evaluated after obtaining an appropriate value for the time instants t_0 and t_1. Then the corresponding histories of $x(t)$ and $y(t)$ can be calculated from Eqs. (8) and (14). This procedure completes the determination of the symmetric periodic solution with a doubly entering saturation region per cycle.

4. Stability of the periodic solutions

Due to the non-smooth non-linearities of magnetic force occurring at the boundaries of the saturation region, the stability of the periodic solution can only be determined by investigating the asymptotic behaviour of perturbations to the steady state periodic solution, as the usual method involving the classical Floquet theory is not applicable to such a non-smooth system.

Let $X(t)$ and $z(t)$ denote the corresponding perturbed solutions to $x(t)$ and $y(t)$, respectively. Performing a similar procedure as used in determining the approximate solution, the first order approximate perturbed solution of the first segment under the perturbed initial conditions, $X(t_0 + \Delta t_0) = -x_s$, $\dot{X}(t_0 + \Delta t_0) = v_0 + \Delta v_0$, can be written as

$$X(t) = X_0(t) + \varepsilon X_1(t) \quad \text{for } |X(t)| \leqslant x_s \tag{17}$$

with

$$X_0(t) = P_1 \sin \Omega\tau + Q_1 \cos \Omega\tau, \tag{18}$$

$$\begin{aligned} X_1(t) = {} & L_1 \sin \Omega\tau + L_2 \cos \Omega\tau + K_1\tau \sin \Omega\tau + K_2\tau \cos \Omega\tau + f_1 t \sin \Omega t \\ & + K_3 \sin 3\Omega\tau + K_4 \cos 3\Omega\tau, \end{aligned} \tag{19}$$

where $\tau = t - t_0 - \Delta t_0$, v_0 represents the initial velocity of the response at time t_0, and the operator, Δ, denotes a small perturbation of the operand. Since the perturbations in the initial conditions are assumed to be small, it is expected that the coefficients in Eqs. (18) and (19) will assume values close to those of the unperturbed motions, respectively [23]. To the first order, the coefficients in Eq. (18) are given by

$$P_1 = P + \Delta v_0/\Omega, \quad Q_1 = Q, \tag{20}$$

where $P = v_0/\Omega$, $Q = -x_s$, are determined by applying the unperturbed initial conditions $X(t_0) = -x_s$, $\dot{X}(t_0) = v_0$, in the corresponding unperturbed solution. The coefficients in Eq. (19) can be expressed as

$$\begin{aligned} L_i &= L_{i0} + l_{i1}\Delta v_0 + l_{i2}\Delta t_0, \quad i = 1, 2, \\ K_j &= K_{j0} + k_{j1}\Delta v_0, \quad j = 1, 2, 3, 4, \end{aligned} \tag{21}$$

where the coefficients L_{i0}, l_{i1}, l_{i2}, K_{j0}, and k_{j1} are defined in Appendix C.

At the time instant, $t = t_1 + \Delta t_1$, the motion of the first segment reaches the upper boundary of the saturation region and will enter the saturation zone thereafter. The perturbed response at the

moment of entrance is assumed to be

$$X(t_1 + \Delta t_1) = x_s, \quad \dot{X}(t_1 + \Delta t_1) = v_1 + \Delta v_1, \tag{22}$$

where v_1 represents the velocity of the unperturbed response of the first segment at t_1.

Substituting Eq. (17) into Eq. (22) and keeping only the first order terms yields

$$\begin{aligned} &a_{11}\Delta t_1 + a_{12}\Delta t_0 + a_{13}\Delta v_0 = 0, \\ &\Delta v_1 = a_{21}\Delta t_1 + a_{22}\Delta t_0 + a_{23}\Delta v_0, \end{aligned} \tag{23}$$

where the coefficients a_{ij} are given in Appendix D.

The asymptotic behaviour of the perturbed motion for the second segment of the response from time $(t_1 + \Delta t_1)$ to $(t_2 + \Delta t_2)$ can be investigated using the same procedure performed as that for the first segment. Similarly, the solution under the perturbed initial conditions, $z(t_1 + \Delta t_1) = \varepsilon^{1/2} x_s$, $\dot{z}(t_1 + \Delta t_1) = \varepsilon^{1/2}(v_1 + \Delta v_1)$, can be written in the form

$$z(t) = P_2 e^{-c(t - t_1 - \Delta t_1)} + Q_2 + m(t - t_1 - \Delta t_1) + G \sin \Omega t + H \cos \Omega t, \tag{24}$$

where the coefficients P_2 and Q_2 are given in Appendix E.

The perturbed response at the time instant $(t_2 + \Delta t_2)$ is assumed to be

$$z(t_2 + \Delta t_2) = \varepsilon^{1/2} x_s, \quad \dot{z}(t_2 + \Delta t_2) = \varepsilon^{1/2}(v_2 + \Delta v_2), \tag{25}$$

where $\varepsilon^{1/2} v_2$ denotes the velocity of the unperturbed response of the second segment at t_2.

Substituting Eq. (24) into Eq. (25), performing some algebraic manipulations and retaining terms up to the first order, yields the following equations:

$$\begin{aligned} &b_{11}\Delta t_2 + b_{12}\Delta t_1 + b_{13}\Delta v_1 = 0, \\ &\Delta v_2 = (b_{21}\Delta t_2 + b_{22}\Delta t_1 + b_{23}\Delta v_1)/\varepsilon^{1/2}, \end{aligned} \tag{26}$$

where the coefficients b_{ij} are defined in Appendix F.

Eqs. (23) and (26) can be expressed in matrix form as

$$\begin{bmatrix} \Delta t_1 \\ \Delta v_1 \end{bmatrix} = R \begin{bmatrix} \Delta t_0 \\ \Delta v_0 \end{bmatrix}, \quad \begin{bmatrix} \Delta t_2 \\ \Delta v_2 \end{bmatrix} = U \begin{bmatrix} \Delta t_1 \\ \Delta v_1 \end{bmatrix}, \tag{27}$$

where R is a 2×2 matrix with elements, $r_{11} = -a_{12}/a_{11}$, $r_{12} = -a_{13}/a_{11}$, $r_{21} = a_{22} - a_{21}a_{12}/a_{11}$, $r_{22} = a_{23} - a_{21}a_{13}/a_{11}$, respectively, and U is a 2×2 matrix with elements, $u_{11} = -b_{12}/b_{11}$, $u_{12} = -b_{13}/b_{11}$, $u_{21} = (b_{22} - b_{21}b_{12}/b_{11})/\varepsilon^{1/2}$, $u_{22} = (b_{23} - b_{21}b_{13}/b_{11})/\varepsilon^{1/2}$, respectively.

The small perturbations of the symmetric solution during the first half-period of the motion are obtained by combining the two equations given by Eq. (27) to form an equation

$$\begin{bmatrix} \Delta t_2 \\ \Delta v_2 \end{bmatrix} = J \begin{bmatrix} \Delta t_0 \\ \Delta v_0 \end{bmatrix}, \tag{28}$$

where J represents the transition matrix for the response from time instant $(t_0 + \Delta t_0)$ to $(t_2 + \Delta t_2)$, and is given by $J = RU$. The stability of the steady state solution is determined by the eigenvalues of this transition matrix. Denoting the trace of J by TJ and the determinant of J by DJ, the two

eigenvalues of the matrix are given by

$$\lambda_{1,2} = \tfrac{1}{2}[TJ \pm (TJ^2 - 4DJ)^{1/2}]. \tag{29}$$

The symmetric period-one motion is asymptotically stable if both eigenvalues λ_1 and λ_2 of matrix J have a modulus less than unity. When either of the two eigenvalues has a modulus greater than one, the solution is unstable. From the proceeding discussion, it may be deduced that all elements of matrix J are functions of the system parameters and the crossing times, which cannot be given explicitly. This means that it is not possible to obtain explicit expressions in terms of the system parameters for the trace and determinant of matrix J. Nevertheless, by substituting the expressions for the elements of matrices R and U and performing some algebraic manipulations, the determinants of matrices R and U, namely DR and DU, may be eventually expressed in a simple form as

$$DR = [1 - \varepsilon(\mu + \delta)t_{10} + O(\varepsilon^2)]\frac{\dot{x}(t_0)}{\dot{x}(t_1)}, \quad DU = \mathrm{e}^{-c(t_2 - t_1)}\frac{\dot{y}(t_1)}{\dot{y}(t_2)}. \tag{30}$$

By imposing continuity and periodicity conditions of the symmetric solution, i.e., $\dot{y}(t_1) = \varepsilon^{1/2}\dot{x}(t_1)$, $\dot{y}(t_2) = -\varepsilon^{1/2}\dot{x}(t_0)$, the determinant of matrix J, as the product of the traces of matrices R and U, is of a quite simple form:

$$DJ = -\mathrm{e}^{-c(t_2 - t_1)}[1 - \varepsilon(\mu + \delta)t_{10} + O(\varepsilon^2)]. \tag{31}$$

Based on the fact that the dimensionless damping coefficient c (i.e., $\varepsilon\mu$) and the dimensionless derivative gain d (i.e., $\varepsilon\delta$) are positive and much smaller than unity for a practical example, and that $|1 - \varepsilon(\mu + \delta)t_{10} + O(\varepsilon^2)| < 1$ always holds, it can be concluded from Eq. (31) that $|DJ| < 1$. This indicates that no Hopf bifurcation is possible in the symmetric motion examined for a practical system. As the system parameters are changed, the modulus of one eigenvalue may take the value of unity, where a bifurcation occurs. One possible way for an eigenvalue to cross the unit circle is through $+1$, which corresponds to a saddle-node, pitchfork or transcritical bifurcation. The other way is through -1, which relates to a period-doubling bifurcation. The stability boundaries $\lambda = \pm 1$ can be established by solving the equation:

$$DJ \mp TJ + 1 = 0. \tag{32}$$

It may be noted that Eq. (32) involves trigonometric and exponential function terms which depend on the crossing times t_1 and t_0. This implies that the stability diagrams cannot be built up analytically. In addition, since the determination of t_1 and t_0 depends on the roots of the two transendental equations given by Eq. (16), a numerical construction of the stability diagrams will be an extremely laborious task. Thus the construction of stability diagrams is not pursued in the present work.

5. Comparison of the approximate and exact solutions

To validate the present analytical results, the symmetric periodic solutions determined by the developed analysis were compared with the exact solutions. The classical fourth order Runge–Kutta algorithm was employed to perform the numerical integration of Eq. (6). It was found that

the approximate solutions obtained by the developed analysis and the exact numerical solutions are in an excellent agreement for the case of primary resonances.

An approximate solution and its stability can be easily constructed and examined using the methodology developed in Sections 3 and 4. For example, in the case $c = 0.1$, $d = 0.3$, $p = 1.4$, $F = 0.4$, $\Omega = 0.65$, and $\varepsilon = 1.0$, the analysis in Section 3 gives that $t_0 = 0.397921$, $t_1 = 1.683299$. The coefficients in Eqs. (12)–(14) can be easily obtained by a back substitution. Then the solution expressions can be easily written out. Two eigenvalues of the transition matrix J for the solution are calculated to be $\lambda_1 = 0.48002$, $\lambda_2 = -0.72654$, which indicates the approximate solution is stable. Fig. 3 shows the phase portraits of the analytical approximate solution and exact solution obtained from numerical integration. The solid curve indicates the results of numerical integration and the circles represent the approximate solution. The differences between the approximate and exact solutions are very small. The approximate solution is in good agreement with the exact solution. The dashed curve in Fig. 3 represents the results of numerical integration of the corresponding linear equation when the non-linearity terms in Eq. (6a) are neglected. It is noted that the solution of the corresponding linear system is not able to be a representation to the solution of the non-linear system.

Fig. 4 shows the maximum amplitudes of the dynamic response of two systems with the variation of the dimensionless proportional gain p in the region $p \in [1.81, 2.21]$, which corresponds to the external detuning in the region $\sigma \in [-0.19, 0.21]$. The system parameters for System I are $d = 0.05$, $c = 0.05$, $F = 0.25$, $\Omega = 1.0$, $\varepsilon = 1.0$, and those for System II are $d = 0.2$, $c = 0.2$, $F = 0.45$, $\Omega = 1.0$, $\varepsilon = 1.0$, respectively. The circles in Fig. 4 indicate values of the amplitudes obtained by the developed analysis and triangles indicate the numerical simulation values. The discrepancies between the first order approximate analytical solutions and exact numerical solutions are between -0.036% and -0.047% for System I, and between 0.504% and 0.741% for System II.

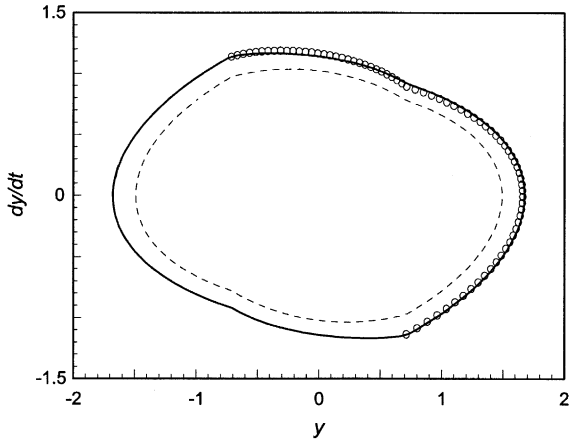

Fig. 3. The phase portraits of the approximate and exact solution; solid curve indicates the direct numerical integration results, circles represent the analytical approximate solution, dashed curve denotes the numerical results of integration of the corresponding linear equations.

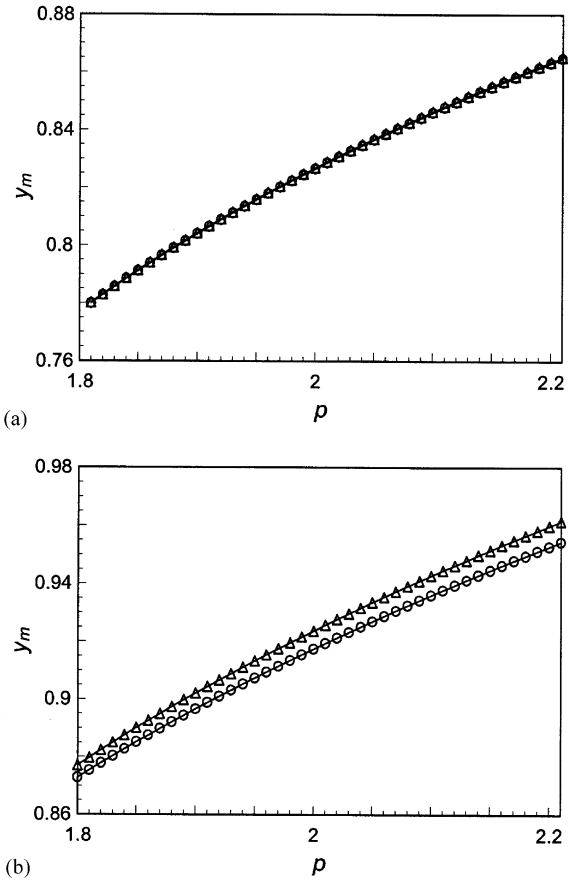

Fig. 4. The variation of the maximum amplitudes of the response of the overall system given by Eq. (6) with the proportional gain p; Circles denote the approximate solutions and triangles represent results of the numerical integration: (a) System I, (b) System II.

Fig. 5 shows the maximum amplitude of the response of Systems III and IV with the variation of the dimensionless forcing frequency in the region $\Omega \in [1.85, 2.15]$, which corresponds to the external detuning in the region $\sigma \in [-0.5775, 0.6225]$. The system parameters for System III are $c = 0.05$, $d = 0.05$, $p = 5.0$, $F = 0.9$, $\varepsilon = 1.0$, and those for System IV are $c = 0.2$, $d = 0.6$, $p = 5.0$, $F = 1.25$, $\varepsilon = 1.0$. The discrepancies between the approximate and exact solutions for System III are between 0.023% and 0.053%, and between 0.468% and 0.578% for System IV. The differences between the approximate and exact solutions for small values of the system parameters are hardly distinguishable by the naked eye (as shown in Figs. 4(a) and 5(a)). For large values of the system parameters, the approximate solutions give slightly smaller values of the maximum response amplitude than those of the exact solutions (as shown in Figs. 4(b) and 5(b)). The first order approximate solutions match well with the numerical exact solutions.

It can be concluded from Figs. 4 and 5 that only small differences between the first order approximate and exact solutions are found. The first order approximate solutions can

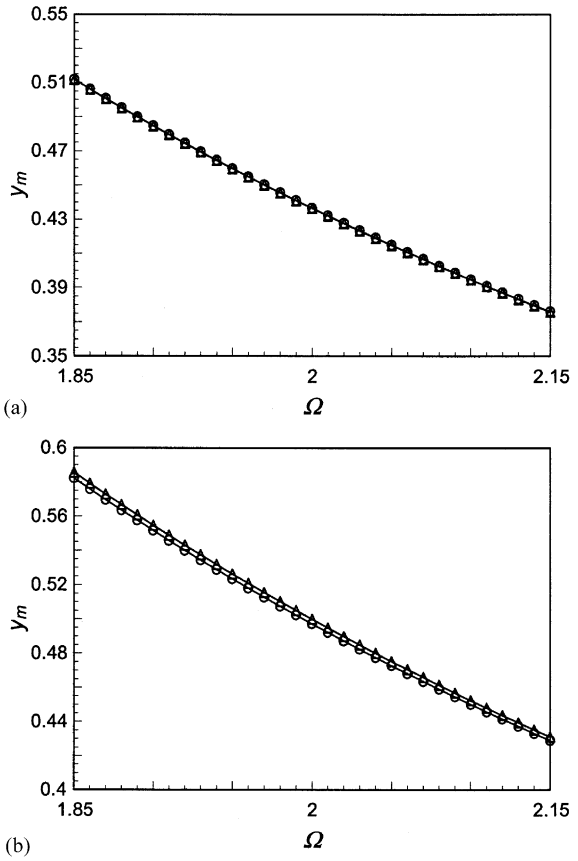

Fig. 5. The variation of the maximum amplitudes of the response of the overall system given by Eq. (6) with the forcing frequency Ω; circles denote the approximate solutions and triangles represent results of the numerical integration: (a) System III, (b) System IV.

give excellent representations of the exact solutions. Additional higher order terms may be included in the approximate solution if a solution of higher accuracy is required, but it seems unnecessary.

6. Conclusion

An approximate periodic solution of a piecewise non-linear–linear oscillator has been analytically determined using a new methodology, as no exact solution exists in closed form. The mathematical model of the oscillator is characterized by a combination of a weakly non-linear and a linear differential equation. More specially, the response of the weakly non-linear system is studied for the case of primary resonances, which may lead to secular terms in the steady state response of a uniformly weakly non-linear system. The methodology developed here involved combining an asymptotic expansion solution to the weakly non-linear system and an

exact solution to the linear system. By imposing an appropriate set of matching and periodicity conditions, the task of determining a periodic symmetric solution with a doubly entering saturation zone per cycle was eventually reduced to a set of two transcendental algebraic equations. The stability characteristic of the symmetric solution was based on examining the propagation of small perturbations in the initial conditions over a half-period of the response. The accuracy of the first order approximate solutions was confirmed by comparison with the results obtained by direct integration of the original equations of motion. More importantly, the methodology developed can be applied to other types of non-smooth systems, which are characterized by different forms of equations of motion.

Acknowledgements

This work was supported by the Australian Research Council under the Discovery-Project Grant DP0343396. The authors would like to thank three anonymous referees for their valuable comments and suggestions.

Appendix A

The coefficients in Eq. (13) are

$$k_1 = -(\mu+\delta)A_1/2 - \sigma B_1/2\Omega - 3\alpha(A_1^2 B_1 + A_1^3)/8\Omega,$$
$$k_2 = -(\mu+\delta)B_1/2 + \sigma A_1/2\Omega + 3\alpha(A_1 B_1^2 + A_1^3)/8\Omega,$$
$$k_3 = \alpha(3A_1 B_1^2 - A_1^3)/32\Omega^2, \quad k_4 = \alpha(B_1^3 - 3A_1^2 B_1)/32\Omega^2, \quad f_1 = f/2\Omega,$$
$$l_1 = -(k_2 + 3\Omega k_3 + f_1 \sin\Omega t_0 + \Omega f_1 t_0 \cos\Omega t_0)/\Omega, \quad l_2 = -k_4 - f_1 t_0 \sin\Omega t_0.$$

Appendix B

The coefficients in Eq. (16) are

$$S_{10} = \sin\Omega t_{10}, \quad C_{10} = \cos\Omega t_{10}, \quad S_{30} = \sin 3\Omega t_{10}, \quad C_{30} = \cos 3\Omega t_{10},$$
$$h_{11} = A_1 + \varepsilon l_1 + \varepsilon k_1 t_{10}, \quad h_{12} = B_1 + \varepsilon l_2 + \varepsilon k_2 t_{10}, \quad h_{13} = \varepsilon f_1 t_1, \quad h_{15} = \varepsilon k_3, \quad h_{16} = \varepsilon k_4,$$
$$h_{21} = \varepsilon^{1/2}(\varepsilon k_1 - \Omega B_1 - \varepsilon\Omega l_2 - \varepsilon\Omega k_2 t_{10}), \quad h_{22} = \varepsilon^{1/2}(\Omega A_1 + \varepsilon\Omega l_1 + \varepsilon k_2 + \varepsilon\Omega k_1 t_{10}),$$
$$h_{23} = \varepsilon^{3/2} f_1 + \Omega H, \quad h_{24} = \varepsilon^{3/2}\Omega f_1 t_1 - \Omega G, \quad h_{25} = -\varepsilon^{3/2} 3\Omega k_4, \quad h_{26} = \varepsilon^{3/2} 3\Omega k_3,$$

with

$$A_1 = [cA_2 e^{-c(\pi/\Omega - t_{10})} - m + \Omega G\cos\Omega t_0 - \Omega H \sin\Omega t_0]/(\varepsilon^{1/2}\Omega), \quad B_1 = -x_s,$$
$$A_2 = [G(\sin\Omega t_0 + \sin\Omega t_1) + H(\cos\Omega t_0 + \cos\Omega t_1) - m(\pi/\Omega - t_{10})]/[e^{-c(\pi/\Omega - t_{10})} - 1],$$
$$B_2 = \varepsilon^{1/2} x_s - A_2 - G\sin\Omega t_1 - H\cos\Omega t_1, \quad t_{10} = t_1 - t_0.$$

Appendix C

The coefficients in Eq. (21) are

$$K_{10} = -(\mu+\delta)P/2 - \sigma Q/2\Omega - 3\alpha(P^2Q+Q^3)/8\Omega,$$
$$k_{11} = -(\mu+\delta)/2\Omega - 3\alpha PQ/4\Omega^2,$$
$$K_{20} = -(\mu+\delta)Q/2 + \sigma P/2\Omega + 3\alpha(PQ^2+P^3)/8\Omega,$$
$$k_{21} = (\sigma + 3\alpha Q^2/4 + 9\alpha P^2/4)/2\Omega^2, \quad K_{30} = \alpha(3PQ^2 - P^3)/32\Omega^2,$$
$$k_{31} = 3\alpha(Q^2-P^2)/32\Omega^3, \quad K_{40} = \alpha(Q^3 - 3P^2Q)/32\Omega^2,$$
$$k_{41} = -3\alpha PQ/16\Omega^3, \quad L_{10} = -(K_{20} + 3\Omega K_{30} + f_1 \sin\Omega t_0 + \Omega f_1 t_0 \cos\Omega t_0)/\Omega,$$
$$l_{11} = -(k_{21} + 3\Omega k_{31})/\Omega, \quad l_{12} = \Omega f_1 t_0 \sin\Omega t_0 - 2f_1 \cos\Omega t_0,$$
$$L_{20} = -K_{40} - f_1 t_0 \sin\Omega t_0, \quad l_{21} = -k_{41}, \quad l_{22} = -f_1 \sin\Omega t_0 - \Omega f_1 t_0 \cos\Omega t_0.$$

Appendix D

The coefficients in Eq. (23) are

$$a_{11} = P\Omega C_{10} - Q\Omega S_{10} + \varepsilon(\Omega L_{10}C_{10} - \Omega L_{20}S_{10} + K_{10}\Omega t_{10}C_{10} + K_{10}S_{10} - K_{20}\Omega t_{10}S_{10} + K_{20}C_{10} + 3\Omega K_{30}C_{30} - 3\Omega K_{40}S_{30} + f_1 \sin\Omega t_1 + \Omega f_1 t_1 \cos\Omega t_1),$$

$$a_{12} = -P\Omega C_{10} + Q\Omega S_{10} + \varepsilon(-\Omega L_{10}C_{10} + \Omega L_{20}S_{10} - K_{10}\Omega t_{10}C_{10} - K_{10}S_{10} + K_{20}\Omega t_{10}S_{10} - K_{20}C_{10} + l_{12}S_{10} + l_{22}C_{10} - 3\Omega K_{30}C_{30} + 3\Omega K_{40}S_{30}),$$

$$a_{13} = S_{10}/\Omega + \varepsilon(l_{11}S_{10} + l_{21}C_{10} + k_{11}t_{10}S_{10} + k_{21}t_{10}C_{10} + k_{31}S_{30} + k_{41}C_{30}),$$

$$a_{21} = -P\Omega^2 S_{10} - Q\Omega^2 C_{10} + \varepsilon(-L_{10}\Omega^2 S_{10} - L_{20}\Omega^2 C_{10} + 2K_{10}\Omega C_{10} - K_{10}\Omega^2 t_{10}S_{10} - 2K_{20}\Omega S_{10} - K_{20}\Omega^2 t_{10}C_{10} - 9K_{30}\Omega^2 S_{30} - 9K_{40}\Omega^2 C_{30} + 2f_1\Omega\cos\Omega t_1 - \Omega^2 f_1 t_1 \sin\Omega t_1),$$

$$a_{22} = P\Omega^2 S_{10} + Q\Omega^2 C_{10} + \varepsilon(L_{10}\Omega^2 S_{10} + L_{20}\Omega^2 C_{10} - 2K_{10}\Omega C_{10} + K_{10}\Omega^2 t_{10}S_{10} + 2K_{20}\Omega S_{10} + K_{20}\Omega^2 t_{10}C_{10} + 9K_{30}\Omega^2 S_{30} + 9K_{40}\Omega^2 C_{30} + l_{12}\Omega C_{10} - l_{22}\Omega S_{10}),$$

$$a_{23} = C_{10} + \varepsilon(l_{11}\Omega C_{10} - l_{21}\Omega S_{10} + k_{11}S_{10} + k_{11}\Omega t_{10}C_{10} + k_{21}C_{10} - k_{21}\Omega t_{10}S_{10} + 3\Omega k_{31}C_{30} - 3\Omega k_{41}S_{30}).$$

Appendix E

The coefficients in Eq. (24) are

$$P_2 = P_0 + A_{21}\Delta t_1 + A_{22}\Delta v_1, \quad Q_2 = Q_0 + B_{21}\Delta t_1 + B_{22}\Delta v_1,$$

where

$$P_0 = (m + \Omega G \cos \Omega t_1 - \Omega H \sin \Omega t_1 - \varepsilon^{1/2} v_1)/c,$$
$$Q_0 = \varepsilon^{1/2} x_s - G \sin \Omega t_1 - H \cos \Omega t_1 - P_0,$$
$$A_{21} = -\Omega^2 (G \sin \Omega t_1 + H \cos \Omega t_1)/c, \quad A_{22} = -\varepsilon^{1/2}/c,$$
$$B_{21} = \Omega[(cH + \Omega G) \sin \Omega t_1 - (cG - \Omega H) \cos \Omega t_1]/c, \quad B_{22} = \varepsilon^{1/2}/c.$$

Appendix F

The coefficients in Eq. (26) are

$$b_{11} = m - cP_0 e^{-c(t_2 - t_1)} + \Omega G \cos \Omega t_2 - \Omega H \sin \Omega t_2,$$
$$b_{12} = B_{21} - m + (cP_0 + A_{21}) e^{-c(t_2 - t_1)}, \quad b_{13} = B_{22} + A_{22} e^{-c(t_2 - t_1)},$$
$$b_{21} = c^2 P_0 e^{-c(t_2 - t_1)} - \Omega^2 G \sin \Omega t_2 - \Omega^2 H \cos \Omega t_2,$$
$$b_{22} = -(c^2 P_0 + cA_{21}) e^{-c(t_2 - t_1)}, \quad b_{23} = -cA_{22} e^{-c(t_2 - t_1)}.$$

References

[1] A.H. Nayfeh, D.T. Mook, *Nonlinear Oscillations*, Wiley, New York, 1979.
[2] P. Hagedorn, *Non-linear Oscillations*, 2nd Edition, Clarendon Press, Oxford, 1988.
[3] J.J. Stoker, *Nonlinear Vibrations in Mechanical and Electrical Systems*, Wiley, New York, 1992.
[4] R.E. Mickens, *Oscillations in Planar Dynamic Systems*, World Scientific, Singapore, 1996.
[5] J.M.T. Thompson, H.B. Stewart, *Nonlinear Dynamics and Chaos*, Wiley, Chichester, 1998.
[6] Y.B. Kim, S.K. Choi, A multiple harmonic balance method for the internal resonant vibration of a non-linear Jeffcott rotor, *Journal of Sound and Vibration* 208 (1997) 745–761.
[7] C.J. Begley, L.N. Virgin, Impact response and the influence of friction, *Journal of Sound and Vibration* 211 (1998) 801–818.
[8] Y. Kang, S.S. Shyr, Y.F. Chang, S.C. Jen, Frequency-locked motion and quasi-periodic motion of a piecewise-linear system subjected to externally nonlinear synchronous excitations, *Journal of Sound and Vibration* 214 (1998) 377–382.
[9] A. Maccari, The response of a forced oscillator under the effect of a pair of set-up elastic stops, *Journal of Sound and Vibration* 235 (2000) 879–887.
[10] S. Natsiavas, S. Theodossiades, I. Goudas, Dynamic analysis of piecewise linear oscillators with time periodic coefficients, *International Journal of Non-Linear Mechanics* 35 (2000) 53–68.
[11] M. Wiercigroch, Mathematical models of mechanical systems with discontinuities, in: M. Wiercigroch, B. de Kraker (Eds.), *Applied Nonlinear Dynamics and Chaos of Mechanical Systems with Discontinuities*, World Scientific, Singapore, 2000, pp. 17–36.
[12] B. de Kraker, J.A.W. van der Spek, D.H. van Campen, Extensions of cell mapping for discontinuous systems, in: M. Wiercigroch, B. de Kraker (Eds.), *Applied Nonlinear Dynamics and Chaos of Mechanical Systems with Discontinuities*, World Scientific, Singapore, 2000, pp. 61–102.
[13] S. Natsiavas, Dynamics of piecewise linear oscillators, in: M. Wiercigroch, B. de Kraker (Eds.), *Applied Nonlinear Dynamics and Chaos of Mechanical Systems with Discontinuities*, World Scientific, Singapore, 2000, pp. 127–159.

[14] J. Warminski, G. Litak, K. Szabelski, Dynamic phenomena in gear boxes, in: M. Wiercigroch, B. de Kraker (Eds.), *Applied Nonlinear Dynamics and Chaos of Mechanical Systems with Discontinuities*, World Scientific, Singapore, 2000, pp. 177–205.
[15] E. Chicurel-Uziel, Exact, single equation, closed-form solution of vibrating systems with piecewise linear springs, *Journal of Sound and Vibration* 245 (2001) 285–301.
[16] E.V. Karpenko, M. Wiercigroch, E.E. Pavlovskaia, M.P. Cartmell, Piecewise approximate analytical solutions for a Jeffcott rotor with a snubber ring, *International Journal of Mechanical Sciences* 44 (2002) 475–488.
[17] S. Lei, A. Palazzolo, A.F. Kascak, Fuzzy logic control of magnetic bearings for suspension of vibration due to sudden imbalance, *Proceedings of the Fifth International Symposium on Magnetic Suspension Technology*, California, 1999, pp. 459–471.
[18] N.M. Thibeault, R. Smith, B. Paden, J. Antaki, Achievable robustness comparison of position sensed and self-sensing magnetic bearing systems, *Proceedings of the Fifth International Symposium on Magnetic Suspension Technology*, California, 1999, pp. 563–573.
[19] G. Schweitzer, H. Bleuler, A. Traxler, *Active Magnetic Bearings, Basics, Properties and Application of Active Magnetic Bearings*, Verlag der Fachvereine (vdf), ETH-Zurich, Switzerland, 1994.
[20] A.H. Nayfeh, *Perturbation Methods*, Wiley, New York, 1973.
[21] E.J. Hinch, *Perturbation Methods*, Cambridge University Press, Cambridge, 1991.
[22] C.F. Chan Man Fong, D. De Chee, *Perturbation Methods, Instability, Catastrophe, and Chaos*, World Scientific, Singapore, 1999.
[23] M.P. Karyeaclis, T.K. Caughey, Stability of a semi-active impact damper: part II, periodic solutions, *American Society of Mechanical Engineers Journal of Applied Mechanics* 56 (1989) 930–940.